

# Microstructure and properties of a bismuth-indium-tin eutectic alloy

S. SENGUPTA, H. SODA, A. McLEAN

*Department of Materials Science and Engineering, University of Toronto,  
184 College Street, Toronto, Ontario, Canada M5S 3E4*

A ternary eutectic alloy with a composition of 57.2%Bi, 24.8%In and 18%Sn was continuously cast into wire of 2 mm diameter with casting speeds of 14 and 79 mm min<sup>-1</sup> using the Ohno continuous casting process. The microstructures and mechanical properties of the wires were compared with those of statically cast specimens. Extensive segregation of massive bismuth crystals, bismuth complex structures, and tin rich dendrites was found in specimens which were statically cast. The bismuth complex-regular structures, which are a ternary eutectic constituent, existed along the boundaries of the BiIn dendrite cells forming a double binary eutectic. In the continuously cast wires, primary tin dendrites coupled with a fine bismuth phase were uniformly distributed within the Bi-In alloy matrix. With this novel, net-shape, casting process, the formation of massive bismuth crystals, bismuth complex-regular structures and BiIn eutectic dendrite cells was prevented, resulting in a more uniform microstructure which was in contrast to the heavily segregated structures of the statically cast specimens. These differences in structure significantly affected the mechanical properties. The continuously cast wires exhibited considerable ductility in contrast with the statically cast specimens which had lower toughness and exhibited cleavage fracture with little or no elongation at higher strain rates.  
© 2002 Kluwer Academic Publishers

## 1. Introduction

Lead and its compounds are known to be toxic and cause severe environmental problems. For this reason, there is an increasing awareness that the use of lead in solder materials should be avoided and there is considerable research being carried out on the development of lead-free solder alloys. Examples of such alloys are Sn-Bi and Sn-Bi-Ag-Cu. However, because of the brittle nature of bismuth and the strong tendency for segregation, alloys with high bismuth concentration are not easily produced in the form of wires and sheets.

Recent work has shown that bismuth can be continuously cast in the form of net-shape wires [1] using the heated mold continuous casting technique known as Ohno Continuous Casting, (OCC) [2]. The results of this investigation suggested that bismuth alloys might also be produced by the OCC technique. If it is applicable, it will open a new way for generating solder and thermal-fuse alloy wires containing high concentrations of bismuth (~50 wt%). Thermal-fuse wires require a diameter of 0.6–0.8 mm in diameter. With the OCC process, wires approximately 1.5–2 mm in diameter can be cast and with the appropriate mechanical properties the cast wires may be further drawn or rolled down to the required sizes. Fig. 1 shows a schematic diagram of the OCC process compared to conventional cooled-mold continuous casting. The OCC technique is a continuous-unidirectional solidification method in which the mold is heated slightly above the solidifi-

cation temperature of the metal to be cast. A cooling device is located a short distance away from the mold exit. Molten metal is introduced continuously into the mold and the solidification front is located just within the mold or just outside the mold depending on the alloys and casting conditions [1, 3].

In the present work, OCC experiments were conducted using the ternary eutectic alloy 57.2 wt%Bi, 24.8 wt%In and 18 wt%Sn which has a melting temperature of 77.5°C. It is noteworthy that the microstructure of this particular alloy was previously studied by Ruggiero and Rutter [4] using specimens which had been unidirectionally solidified at very slow speeds of 0.74–53 mm day<sup>-1</sup>. So this alloy composition was chosen to represent the materials of high bismuth concentration.

Material of the same composition was also produced by a static casting method in which the specimens were melted and solidified within the furnace, and the microstructures and mechanical properties compared with those of the continuously cast wires. This information may help in assessing the suitability of the OCC process as an alternative method for producing low temperature solder as well as thermal-fuse alloy wires.

## 2. Experimental aspects

Fig. 2a shows a schematic diagram of the melting and casting arrangement designed to apply the principle of the OCC process [2] to the generation of small wires

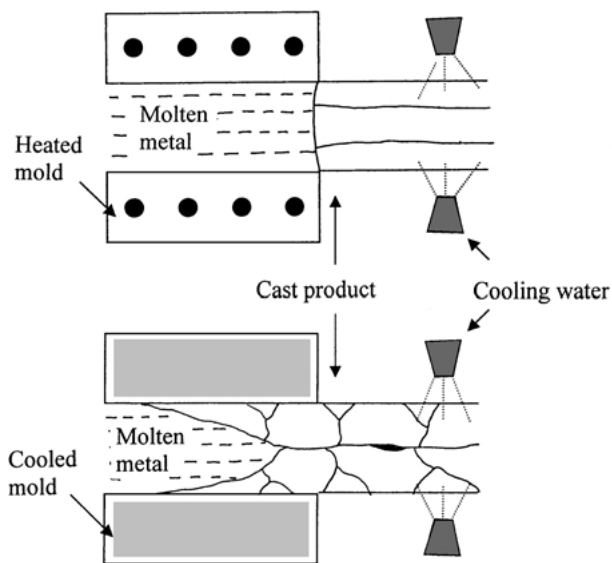


Figure 1 Schematic diagram of the OCC heated mold process in contrast to the conventional cooled mold continuous casting technique.

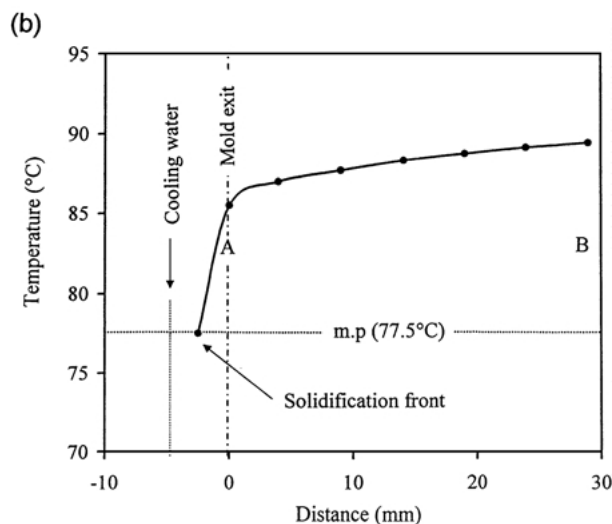
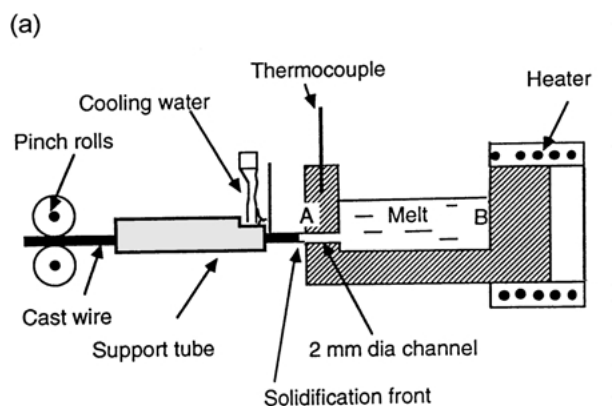


Figure 2 (a) Schematic diagram of the melting and continuous casting arrangement. (b) Temperature distribution within the melt from point A to point B.

1.5–2 mm in diameter. The equipment consists of a melting facility for approximately 15 g of alloy, a cooling device, a support tube for minimizing mechanical instability, and pinch rolls for withdrawal of cast wires. The melt temperature was maintained at about 87–90°C. The cooling water was positioned approximately

5 mm away from the mold exit when casting at a speed of 14 mm min<sup>-1</sup> and at a closer distance for a higher casting speed (79 mm min<sup>-1</sup>). Fig. 2b shows the temperature distribution within the melt from point A to the mold exit, Fig. 2a, during the casting of wire at a speed of 14 mm min<sup>-1</sup>. With this speed, the solidification front was located midway between the cooling water and mold exit creating the liquid column supported by surface tension. This condition provides a cooling rate of approximately 45°C min<sup>-1</sup>. Continuously cast specimens used for mechanical testing were produced at a casting speed of 79 mm min<sup>-1</sup>. In this case, the cooling position was closer to the mold (~4 mm) to maintain the solidification front at approximately 2 mm from the mold exit. This provided wires with a better dimensional stability. The cooling rate was calculated to be 253°C min<sup>-1</sup> assuming the temperature gradient in Fig. 2b remains the same. During casting, alloy granules were fed periodically into the holding container to maintain a constant metal head.

For comparison purposes, the Bi-In-Sn alloy wires produced by the continuous casting process were used as melt stock for fabrication of ~100 mm long, statically cast specimens solidified either in a glass tube or graphite split-mold placed within the furnace. About 7 g of the alloy wire was melted in a glass tube 3.2 mm ID located within a vertical furnace. After melting, the furnace assembly with the glass tube containing the alloy specimen was positioned horizontally for solidification. Fig. 3 shows a temperature profile within the furnace which has a temperature plateau region approximately 60 mm long and a temperature gradient region (~0.5°C mm<sup>-1</sup>) approximately 30 mm long. The alloy specimen was allowed to solidify slowly by switching off the power to the furnace. The temperature profiles

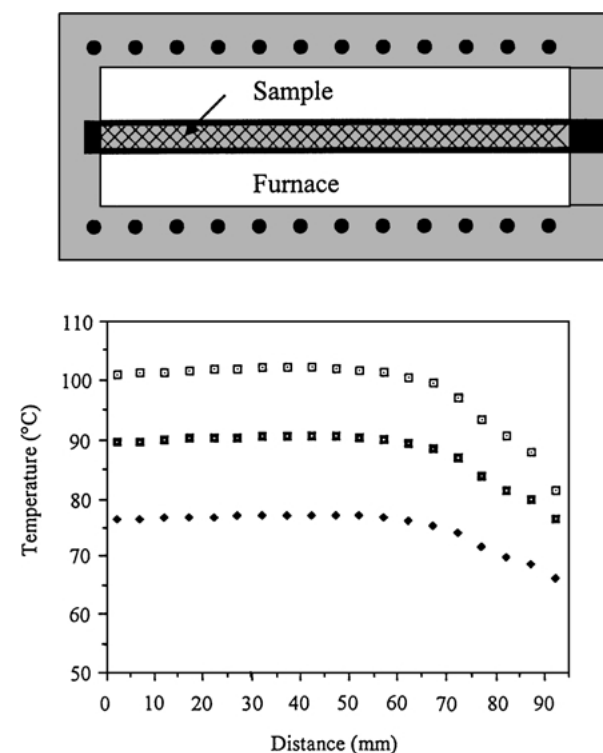


Figure 3 Furnace and specimen assembly used for static solidification together with temperature profiles within the furnace at three different temperature settings.

at different furnace temperature settings represent the subsequent temperature distribution during the cooling period of the specimen. This temperature distribution facilitated a directional and non-directional solidification within the specimen the microstructures of which were compared with those of specimens produced by continuous casting. Temperature was also monitored during cooling by means of a chromel-alumel thermocouple attached to the glass mold containing the specimen, located in the uniform temperature zone of the furnace. The average temperature drop before reaching the eutectic temperature was approximately  $1^{\circ}\text{C min}^{-1}$ . When the temperature reached  $55^{\circ}\text{C}$  the specimen was taken out of the furnace and cooled in air.

Statically cast specimens for mechanical testing were solidified within a graphite split-mold placed within the furnace, which provided a uniform temperature distribution along the length of the specimen. Specimens solidified within the furnace and those produced by the continuous casting process are referred to as “statically cast specimens” and “continuously cast specimens” respectively.

The eutectic alloy was prepared from the elemental metals of 99.99% purity melted together in a graphite crucible under an argon atmosphere. The molten alloy was quenched in a water bath to produce granules which were subsequently used as melt stock for the generation of continuously cast wires. Metallographic samples were lightly etched for approximately 30 seconds with a dilute solution (10% strength) of the following reagent: water 300 ml,  $\text{K}_2\text{CrO}_7$  6 g,  $\text{H}_2\text{SO}_4$  20 ml, NaCl (saturated solution) 12 ml, HF 80 ml, and  $\text{HNO}_3$  40 ml [5].

In order to characterize the material properties of specimens produced by the above methods, tensile tests were performed at room temperature. Statically cast specimens for mechanical testing were machined to a gauge length of 25 mm and diameter of approximately 2 mm. Each specimen was machined until visible surface defects were eliminated along the gauge length. Although the surface of continuously cast specimens was smooth, they were also machined in order ensure that the surface condition was equivalent to that of the statically cast specimens.

### 3. Results and discussion

#### 3.1. Microstructure of statically cast alloys

Although a detailed account of the microstructure of this eutectic alloy was described elsewhere [6], the microstructural differences which contributed to a significant difference in the mechanical behavior of the cast products were only briefly described. From the ternary phase diagram of Bi-In-Sn [4], the equilibrium eutectic constituents should be  $\gamma\text{Sn}$ , BiIn, and Bi phases. However for statically cast specimens, as shown in Fig. 4, the microstructure consisted of regions of eutectic grains (gray), mottled tin-rich dendrites (black), bismuth blocks (white), and skeletal structures of bismuth similar to the complex regular structures observed in the binary eutectic systems of Bi-Sn and Bi-Pb [7–9]. For this reason, they are also referred to in this work as complex regular structures. Using energy dispersive X-ray analysis, (EDX), it was found

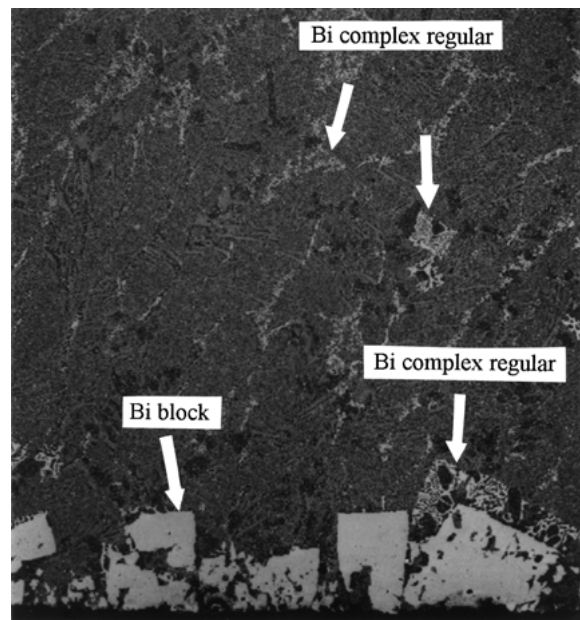


Figure 4 Backscattered SEM image of a statically cast specimen solidified within a graphite mold showing extensive gravity segregation of block-like bismuth phase and the growth of bismuth complex regular structure.

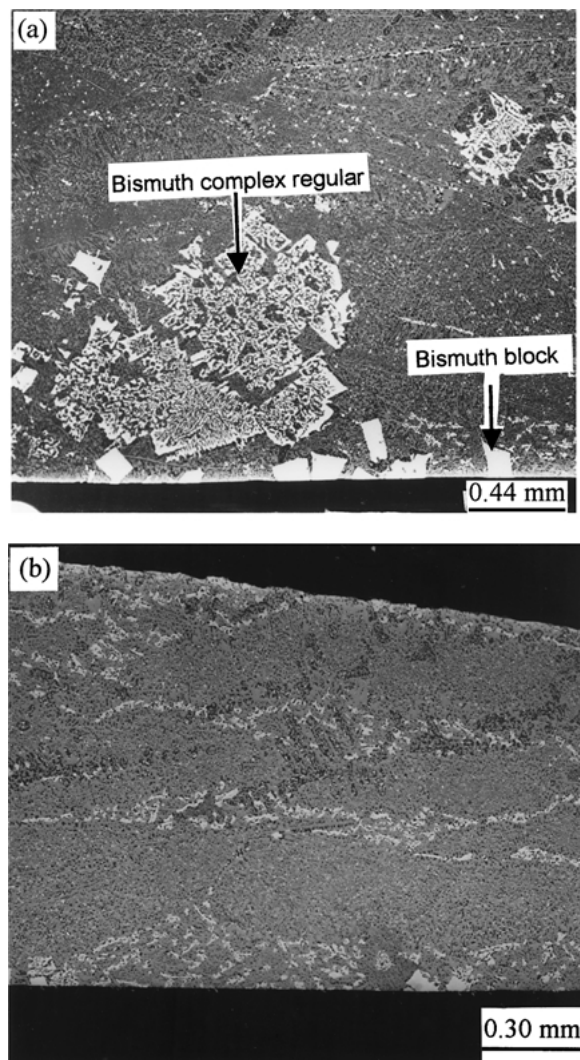


Figure 5 Backscattered SEM images of longitudinal section of a statically cast specimen (a) from the temperature plateau region showing massive growth of a complex regular structure of bismuth (white) and (b) from the temperature gradient region showing directional structure and less segregation.

that the bismuth phase was pure bismuth, the tin phase contained a small amount of bismuth and indium, and the gray matrix within the eutectic grains contained bismuth, indium, and a small amount of tin, which is essentially the same as that identified as BiIn with some solubility of bismuth and tin by Ruggiero and Rutter [4], who investigated the microstructure of the same alloy.

The most notable aspect of the microstructures in the statically cast specimens was that they exhibited extensive gravity segregation involving massive blocks of bismuth and the large skeletal structures of bismuth, indicated by an arrow in Fig. 4. Similar gravity segregation structures have been reported for a Sn-Pb alloy of eutectic composition in which lead primary dendrites nucleated in the undercooled melt and segregated to the lower part of the ingot while tin rich dendrites nucleated in the upper region, producing a compositional gradient and creating an ingot with a mixture of phases other than the eutectic in the final solidified structure [10]. The massive complex regular structures of Bi were more frequently observed (Fig. 5a) in specimens

solidified within the glass mold situated in the temperature plateau region of the furnace compared to those solidified in the graphite mold, suggesting that subtle differences in solidification conditions affect the morphology of the bismuth phase. A section of the specimen solidified within the temperature gradient region of the glass mold exhibited a unidirectional structure and less segregation (Fig. 5b). In all cases, the complex regular structure of bismuth tended to segregate between the eutectic grains and in addition, bismuth blocks were occasionally trapped between them. Examples of these structures are shown in Fig. 6.

As mentioned previously, Ruggiero and Rutter [4] carried out a detailed study in which the Bi-In-Sn ternary eutectic alloy was solidified unidirectionally under very slow growth rate conditions ( $0.74\text{--}53\text{ mm day}^{-1}$ ). The alloy exhibited a marked tendency to form two distinct binary eutectic structures rather than a ternary eutectic structure with a repetitive arrangement of three phases. This “double binary microstructure” consists of regions of a quasi-regular BiIn- $\gamma$ Sn binary

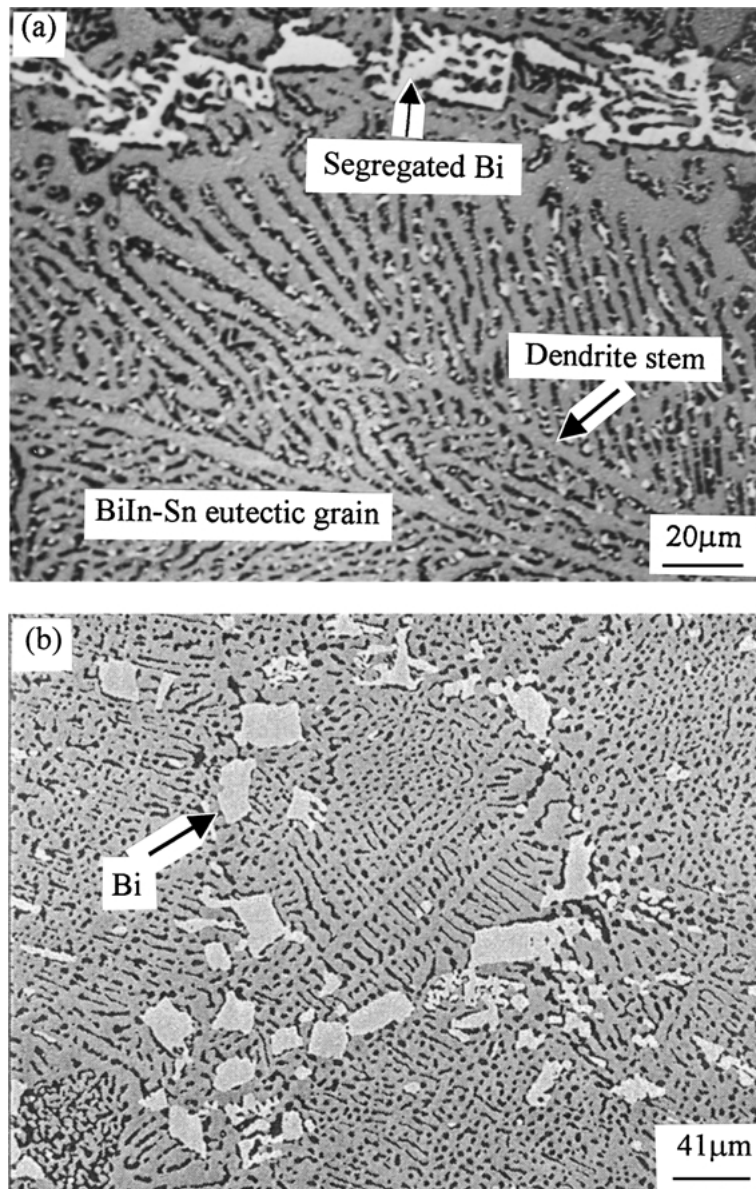


Figure 6 BiIn-Sn eutectic grains and segregation of the bismuth complex regular structures (a) and bismuth blocks (b) along the eutectic grain boundaries in statically cast specimens.

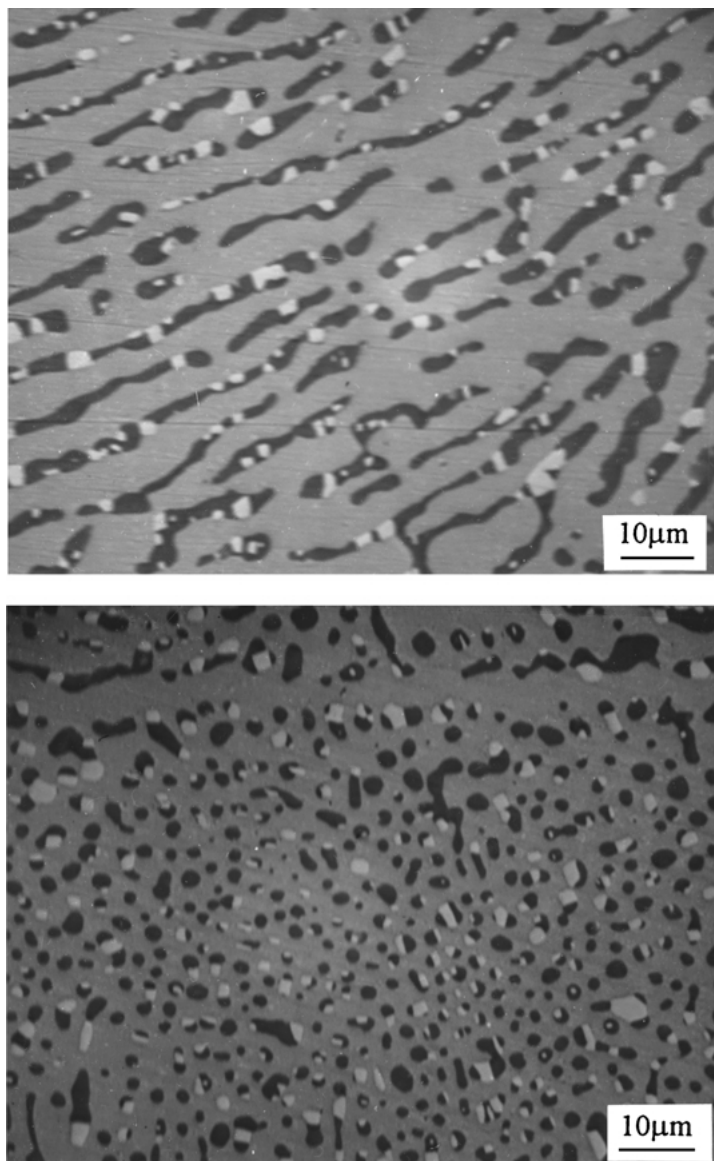


Figure 7 Morphology of Sn phase (dark) observed within the BiIn-Sn eutectic grains in a statically cast specimen exhibiting lamellae and rod type forms. The Bi phase (white) formed due to decomposition of the  $\gamma$ Sn.

eutectic as well as regions of Bi- $\gamma$ Sn binary eutectic in a complex-regular form. The  $\gamma$ Sn decomposed on cooling to form Bi, BiIn and  $\beta$ Sn.

In the present investigation, although the growth rate under statically cast conditions ( $\sim 2 \text{ mm min}^{-1}$  in the temperature gradient region) is much faster than those employed by Ruggiero and Rutter, it was found that the alloy also formed a double binary structure. In this case however, the BiIn-Sn binary eutectic grew in a dendrite form in which the BiIn dendrite stems and arms can be clearly seen (Fig. 6) and Bi-Sn binary eutectic grew in the form of a complex regular structure that segregated between the BiIn-Sn eutectic grains to compose a double binary eutectic structure. As shown in Fig. 7, the morphology of the tin phase that occupies the interdendritic region of the BiIn-Sn eutectic colony was lamellar and rod type dotted with bismuth particles due to decomposition.

### 3.2. Microstructure of continuously cast alloys

Since the Ohno continuous casting process in the present work involves the water-cooling of cast wires

approximately 2 mm from the solidification front, a fine microstructure is expected. Fig. 8 shows backscattered SEM micrographs of the longitudinal and transverse sections of a continuously cast wire and it is evident that the structure is much more uniform compared to the heavily segregated structures of statically cast specimens. The structure consists of a Bi-In alloy matrix phase (gray) in which tin primary dendrites (black), associated with small bismuth particles (white), are uniformly distributed, with tin particles dispersed between the dendrites. This structure is distinctly different from those observed in the statically cast samples. There was no formation of massive bismuth blocks, bismuth complex-regular cells, BiIn dendrite cells or of double binary eutectic structures in the continuously cast wires. Furthermore, there was no evidence of bismuth segregation.

For casting speeds of 14 and 79  $\text{mm min}^{-1}$ , the phases and morphologies observed were essentially similar with the only difference being in the degree of fineness of the cast structures. For example, the secondary dendrite arm spacings of the tin phase, as measured by a line intercept method, were approximately 9  $\mu\text{m}$  and

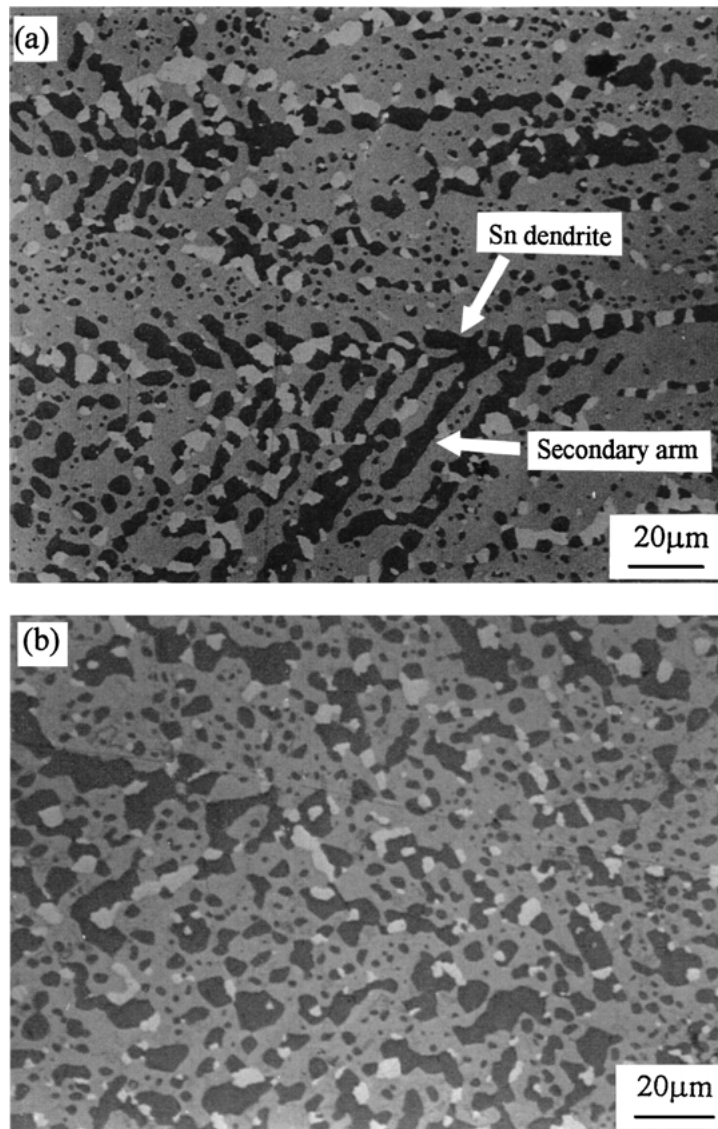


Figure 8 Microstructure of an OCC specimen cast at  $14 \text{ mm min}^{-1}$ : (a) longitudinal and (b) transverse sections showing the dispersions of bismuth phase (white).

$3 \mu\text{m}$  respectively. In contrast, the dendrite arm spacing of the tin phase in statically cast specimens from the temperature gradient region was approximately  $30 \mu\text{m}$  at a growth speed of approximately  $2 \text{ mm min}^{-1}$ . Thus the microstructures of the continuously cast wires are on the order of 3 to 10 times finer than those of the statically cast specimens.

**3.3. Mechanical properties of the cast alloys**  
As noted above there are significant differences in structural morphology between the statically cast and continuously cast specimens. In general, the statically cast specimens exhibited a coarse polycrystalline microstructure in which the bismuth phase segregated in a block-like form at the bottom of the specimen due

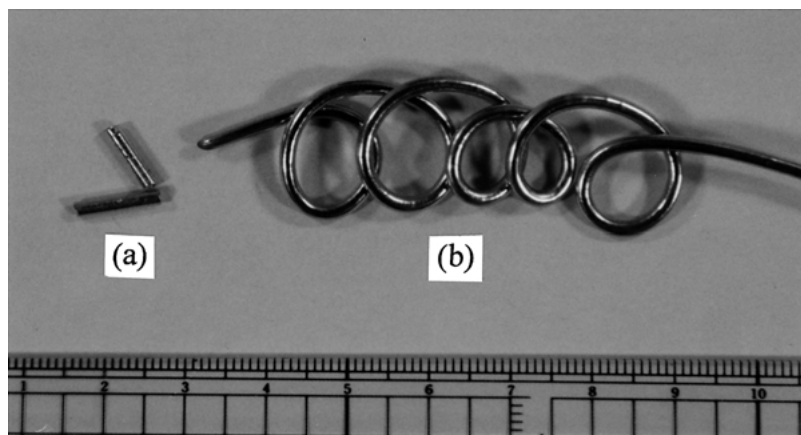


Figure 9 (a) Statically cast and (b) continuously cast specimens exhibiting difference in ductility.



to gravity as well as in the form of a complex regular structure along the BiIn-Sn eutectic grain boundaries. On the other hand, the continuously cast specimens exhibited a much finer and more uniform microstructure within which was dispersed a small discrete bismuth phase. These differences were reflected in the mechanical properties. For example, as shown in Fig. 9, statically cast specimens were easily fractured, whereas the continuously cast specimens exhibited considerable ductility. Also, another striking difference was that turning chips generated during machining of statically cast specimens were finely fragmented, whereas those of continuously cast specimens formed long ribbon-like strips. The fragmentation of turnings is most likely due to the segregation of Bi phase along the grain boundaries.

Fig. 10 shows the microstructure of statically cast rod at the location where the rod was mechanically sheared. It was found that bismuth in the form of large block and complex regular structures were associated with cracks, fragmentation, and decohesion while the small bismuth particles ( $\sim 5 \mu\text{m}$ ), which existed within the BiIn-Sn eutectic grains, were unaffected by the deformation. There are cracks formed within the bismuth block and the complex structure of bismuth (Fig. 10a) as well as cavities caused by decohesion along the bismuth-eutectic grain interface (Fig. 10b). These suggest that the large bismuth phases play an active role in the formation of cracks. In the brittle fracture mode, the nucleation of cracks is the crucial step, whereas in the ductile fracture mode crack propagation becomes important [11]. The dispersion of bismuth as small discrete particles in

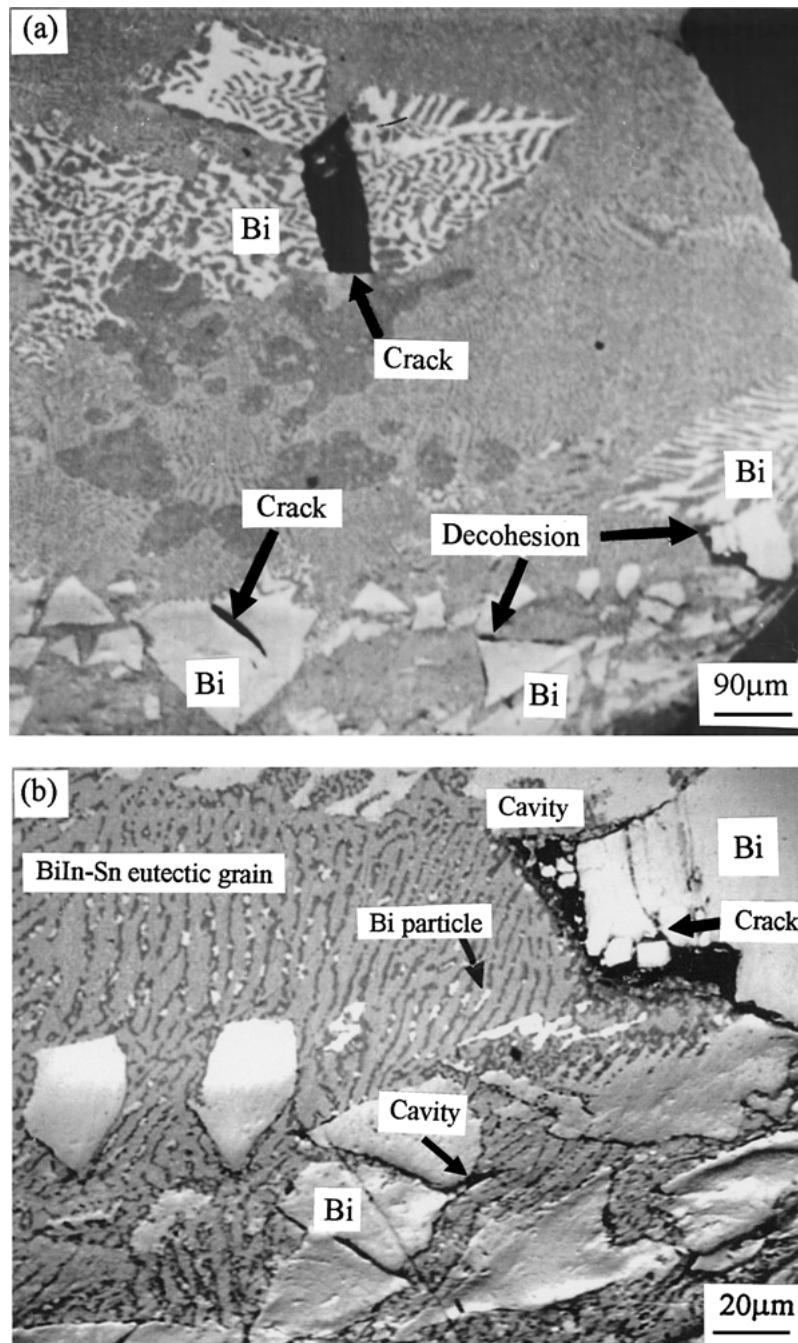


Figure 10 Micrographs of statically cast specimen (a) showing cracks within the bismuth block and the complex regular structure of bismuth and (b) showing cavities (dark area) due to decohesion of the interface between bismuth block and BiIn-Sn eutectic grain as well as cracks and fragmentation of bismuth block.

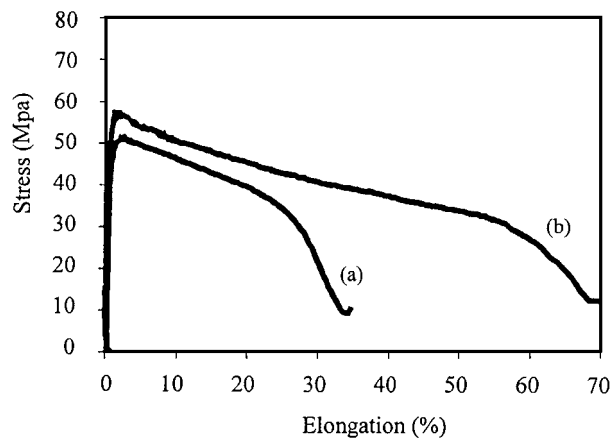


Figure 11 Stress-strain curves obtained for (a) statically cast and (b) continuously cast specimens at a crosshead speed of  $2.5 \text{ mm min}^{-1}$ .

continuously cast alloys (Fig. 8) will be less prone to act as sites for crack initiation, thus leading to significant differences in the mechanical properties.

Tensile tests were performed for both specimens at crosshead speeds between  $1.25 \text{ mm min}^{-1}$  and  $10 \text{ mm min}^{-1}$ , which corresponds to an initial strain-rate between  $8.33 \times 10^{-4} \text{ s}^{-1}$  and  $6.66 \times 10^{-3} \text{ s}^{-1}$ . From stress-strain tests, Fig. 11, the values of yield stress, ultimate tensile strength (UTS), elongation and reduction in area were obtained, Fig. 12. In this figure each value is the average of three tests. The values of yield stress for continuously cast specimens are consistent and independent of the cross-head speed in contrast to the behavior observed with statically cast specimens which exhibited a large scatter and abrupt decrease in value at crosshead speed above  $5 \text{ mm min}^{-1}$ .

The values of UTS for continuously cast specimens appear to increase slightly with the crosshead speed while those for statically cast specimens exhibited a trend consistent with that observed for the yield stress. The large difference between maximum and minimum values of UTS for statically cast specimens at higher crosshead speeds ( $7.5$  and  $10 \text{ mm min}^{-1}$ ) suggests that the fracture may be a stochastic occurrence since the statically cast specimens contain inherent microstructural weaknesses including the presence of large primary Bi blocks and a eutectic Bi phase along the grains, and voids (casting defects) associated with the eutectic Bi phase. Fracture could be initiated by any of these factors. On the other hand, continuously cast samples showed no indication of premature fracture, even at the highest crosshead speed of  $10 \text{ mm min}^{-1}$ .

Continuously cast specimens exhibited elongation values ranging from 30 to 73% of initial gage length, whereas the statically cast specimens had values within 0.5% and 43%. From the plot of elongation versus crosshead speed, it is clear that at all crosshead speeds from  $1.25$  to  $10 \text{ mm min}^{-1}$ , continuously cast samples exhibited higher average elongation compared to statically cast specimens and the values decreased only slightly with cross-head speed. The statically cast specimens showed ductile fracture up to the crosshead speed of  $5 \text{ mm min}^{-1}$  with an average elongation of approximately 30%. At the crosshead speed of  $7.5 \text{ mm min}^{-1}$

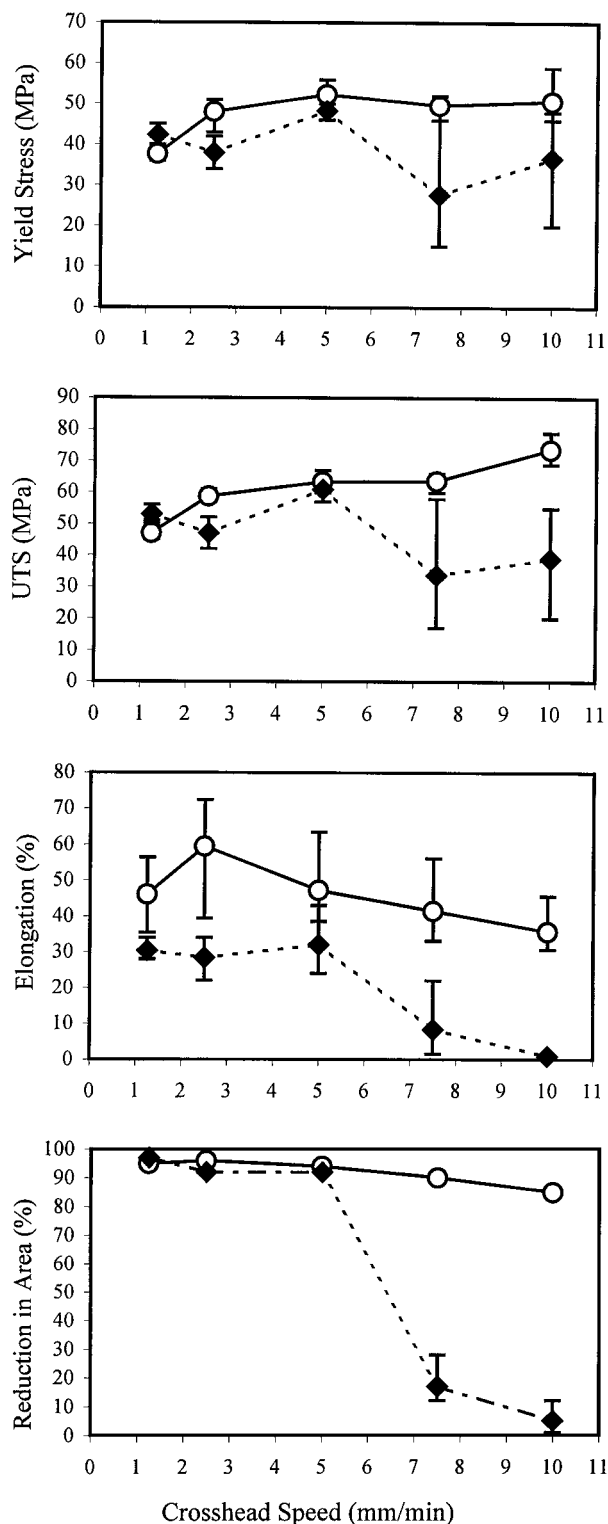


Figure 12 Change in values of yield stress, UTS, elongation, and reduction in area with crosshead speed for continuously cast (O) and statically cast (◆) specimens. Each value represents the average of 3 tests.

the specimens tended to exhibit brittle fracture resulting in a sharp decrease in elongation and at  $10 \text{ mm min}^{-1}$ , exhibited almost no elongation. This ductile to brittle fracture transition is more clearly seen in reduction in area which indicates a significant decrease in value above crosshead speeds of  $5 \text{ mm min}^{-1}$ .

Glazer [12] in his review on the properties of low temperature lead-free solder alloys suggested that although ductility of the solder joints decreases with increasing strain rate for the Sn-Bi eutectic alloy, the considerable



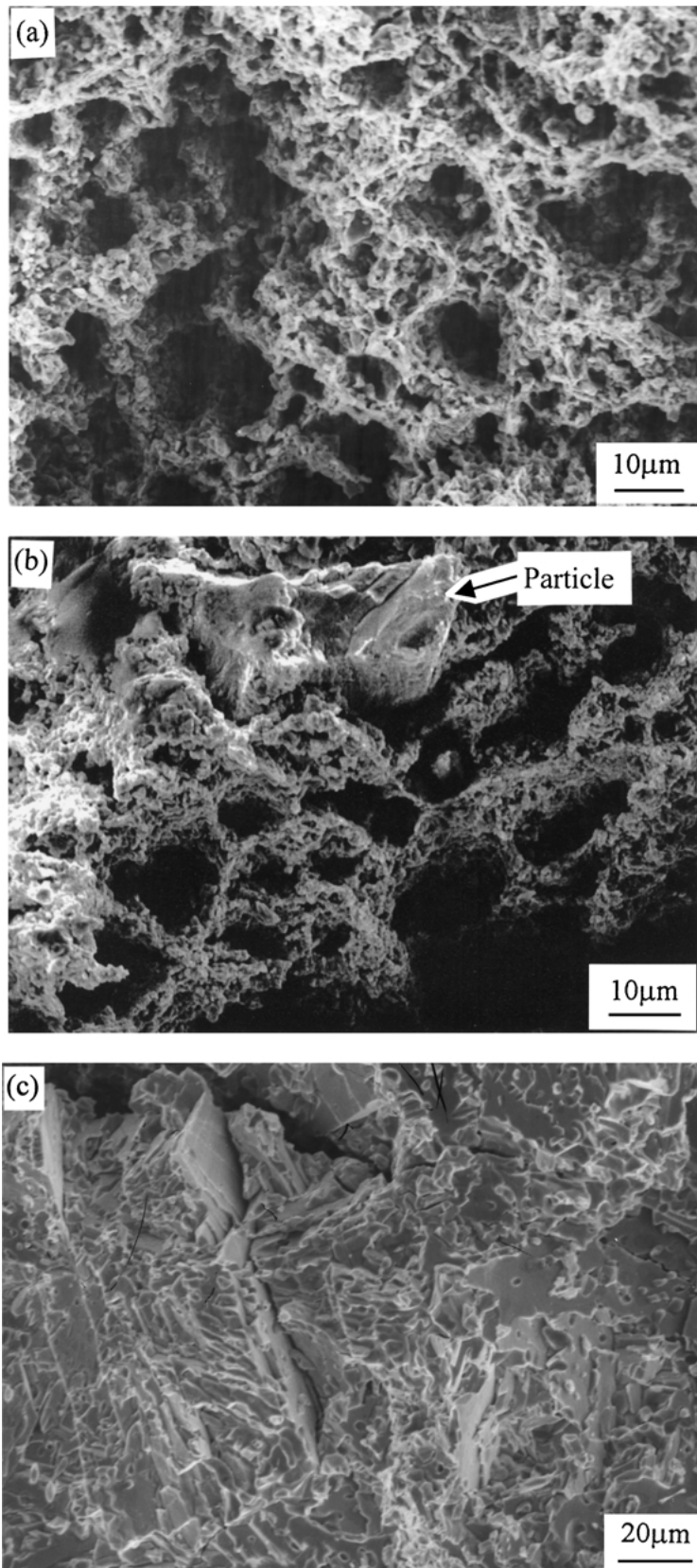


Figure 13 Fracture surfaces of (a) continuously cast specimen tested at a crosshead speed of  $5 \text{ mm min}^{-1}$  and (b, c) statically cast specimens tested at a speed of  $1.25 \text{ mm min}^{-1}$  and  $10 \text{ mm min}^{-1}$  respectively.

differences among the values reported by the various investigators might be due to the microstructural differences of tested specimens.

### 3.4. Fracture behaviour

Fig. 13 shows the fracture surfaces of continuously cast and statically cast specimens. Within the crosshead

speed range of  $1.25$  to  $10 \text{ mm min}^{-1}$ , the fracture surface of OCC specimens show similar ductile fracture features with a spongy appearance due to voids and small dimples. The fracture surfaces of statically cast specimens for crosshead speeds up to  $5 \text{ mm min}^{-1}$  were essentially similar to those of continuously cast specimens. However, there were large fragmented

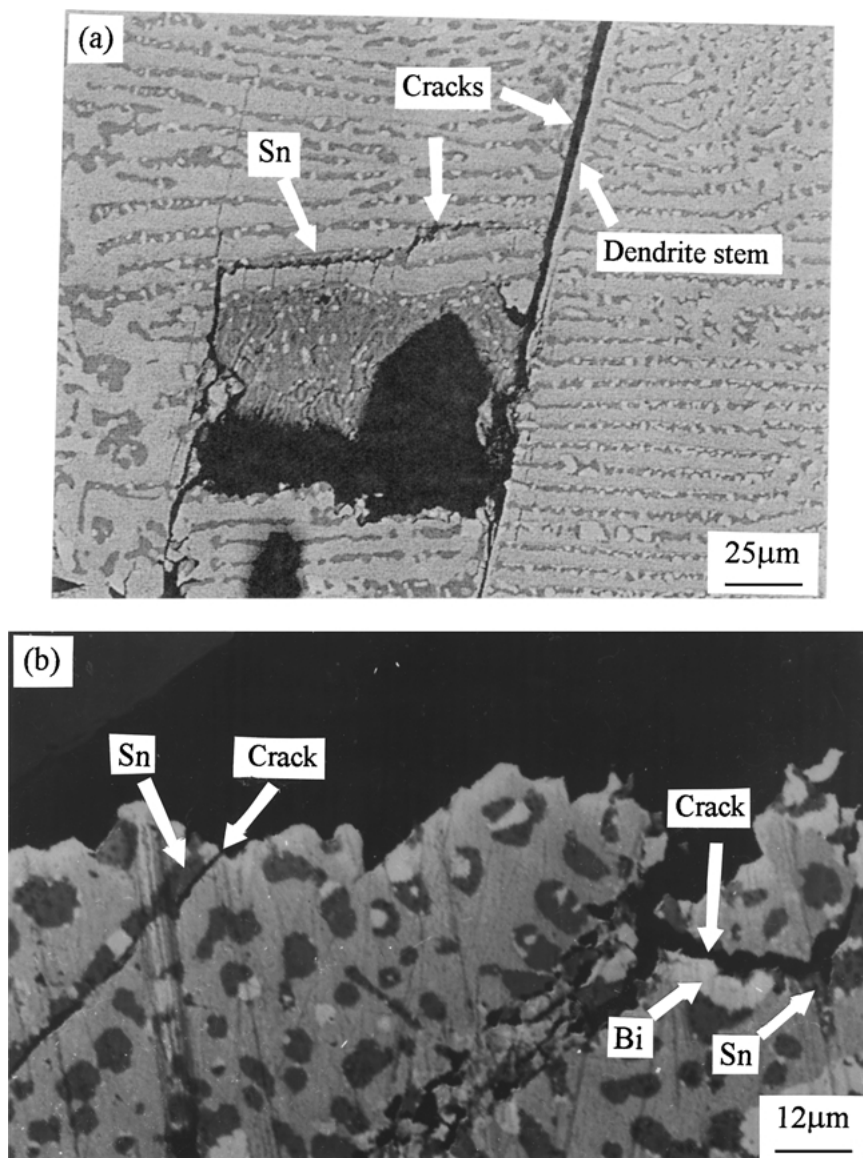


Figure 14 Statically cast specimens showing the trans-granular crack propagation (a) within BiIn dendrite stem and along tin lamellae and (b) along the bismuth-matrix interface and also along the tin-matrix interface.

bismuth particles protruding from the fractured surface (Fig. 13b). At higher crosshead speeds ( $7.5$  and  $10 \text{ mm min}^{-1}$ ), statically cast specimens exhibited cleavage fracture with little or no ductility (Fig. 13c). Although ductile fracture behavior was observed up to a crosshead speed of  $5 \text{ mm min}^{-1}$  for the statically cast specimens, areas below the stress-strain curves (Fig. 11) were about 1.3 to 2.3 times smaller than those of continuously cast specimens, indicative of a lower toughness.

Material failure generally occurs in the tensile mode by interruption of plastic deformation with the development of voids or cracks at the particle-matrix interface. In this Bi-In-Sn eutectic composition, the phases observed are tin, bismuth, and Bi-In matrix. Cavities or cracks may initiate at the interface of bismuth-matrix, tin-matrix, or tin-bismuth, or at more than one interface at the same time.

In order to identify which interface plays the more active roll in the generation of decohesion, some of the fractured specimens were examined using electron microscopy, Fig. 14a shows fissures observed within the BiIn-Sn eutectic grains of a statically cast speci-

men that fractured in a brittle manner. The fissure ran linearly along the length of the dendrite stem within the grain and the other fissure propagated along the tin lamellae some distance before crossing to the adjacent tin lamellae. Also shown in Fig. 14b are the cracks observed at the edge of the brittle-fractured surface of the tensile specimen. There was decohesion along the bismuth-matrix interface and also along the tin-matrix interface. These are indicative of the fact that the bismuth-matrix and the tin-matrix interfaces in this alloy are a potential source of weakness, which can lead to trans-granular fracture (Fig. 13c). Longitudinal cross-sections of the necked region of test specimens were also examined. Fig. 15 shows the backscattered SEM images of the fracture region of specimens tested at the crosshead speed of  $2.5 \text{ mm min}^{-1}$ . For the statically cast specimens (Fig. 15a and b), although small voids occur at the tin-matrix interface it was found that large voids were directly associated with the blocks of bismuth phase clearly indicating that decohesion at the bismuth-matrix interface can play a significant role in crack initiation. These observations suggest that for

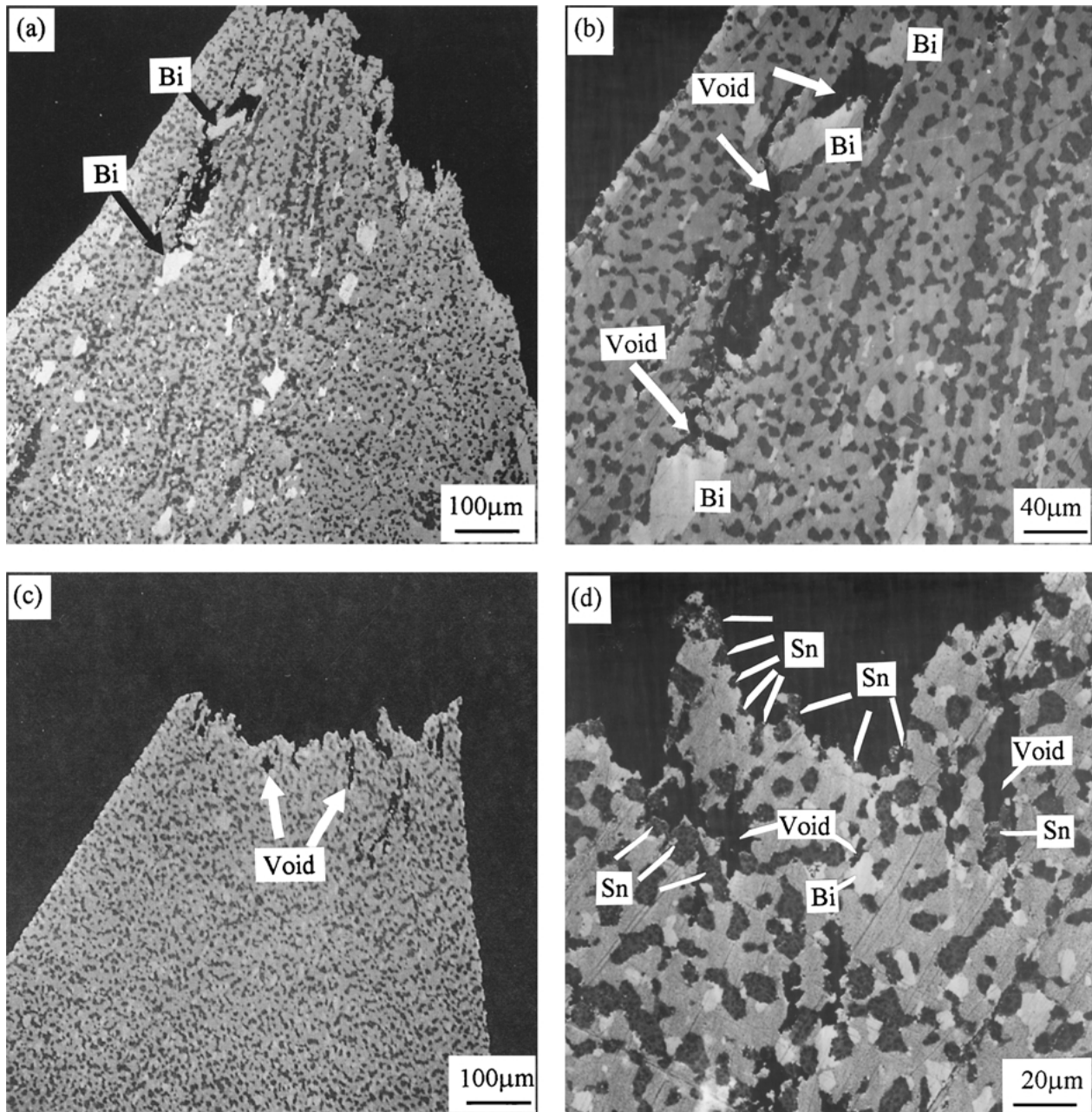


Figure 15 Void formation at the fracture location of specimens tested at a crosshead speed of  $2.5 \text{ mm min}^{-1}$ , showing voids associated with large bismuth phases in a statically cast specimen (a, b) and voids which originated preferentially at the tin-matrix interface in a continuously cast wire (c, d).

statically cast specimens the voids preferentially initiate at the surface of large bismuth particles. In contrast, for continuously cast specimens, due to the absence of large bismuth particles, the voids were more uniformly distributed within the necked region (Fig. 15c) and decohesion appeared to occur mainly at the tin-matrix interface (Fig. 15d) and to lesser extent, at the bismuth-matrix interface. From observation of the edge of the fracture surface (Fig. 15d) it appears that the cracks propagated by following the tin phase resulting in the fracture texture with a sponge-like appearance.

Large concentration of bismuth blocks due to gravity segregation found in statically cast material (Figs 4 and 10) will exert an adverse effect on the mechanical properties. For this reason, this layer was eliminated during machining of the surface of test specimens. However, the bismuth phases that exist between the eutectic grains are still significantly larger compared to the bismuth particles within the grains (Figs 6 and 7).

Thus, stress concentration at the large bismuth particles will be much greater leading to crack formation and, in combination with a high strain rate, crack propagation in the trans-granular brittle fracture mode as shown in Fig. 13c.

#### 4. Summary

An experimental study was conducted in order to investigate the applicability of the OCC process for the generation of Bi-In-Sn ternary eutectic alloy wires. The microstructures and mechanical properties of the continuously cast wires were compared with those of statically cast specimens. The results are summarized as follows:

1. It has been established that Bi-In-Sn ternary eutectic alloy wires of  $\sim 2 \text{ mm}$  diameter with uniform structures can be continuously cast by the OCC process.

2. Alloy which was statically cast exhibited extensive macrosegregation of massive bismuth crystals, bismuth complex structures and tin-rich dendrites.

3. Statically cast specimens of ternary eutectic composition exhibited a double binary eutectic structure, consisting of regions of BiIn dendrite cells and regions of bismuth complex-regular cells.

4. In the case of wires produced by continuous casting at speeds of 14 and 79 mm min<sup>-1</sup>, a uniform microstructure was observed in contrast to the heavily segregated structures of the statically cast specimens.

5. In continuously cast wires, bismuth was dispersed uniformly as fine discrete crystals within a structure in which massive bismuth crystals, bismuth complex-regular cells, and BiIn dendrite cells were absent.

6. Large cavities formed at the interface between large bismuth crystals and the matrix in fractured statically-cast specimens are indicative of the fact that fracture can be initiated at the segregated bismuth particles. In the case of continuously cast wires, due to the absence of large bismuth particles void formation mainly occurred at the interface between fine tin particles and the matrix. It is suggested that this difference in void nucleation may contribute to the differences in mechanical properties.

7. Continuously cast wires exhibited ductile behaviour over the full range of initial strain rates evaluated, i.e.  $8.33 \times 10^{-4}$  to  $6.66 \times 10^{-3}$  s<sup>-1</sup>. In contrast, statically cast specimens showed little or no ductility in the range of higher strain rates, i.e.  $5 \times 10^{-3}$  to  $6.66 \times 10^{-3}$  s<sup>-1</sup> and failure occurred by trans-granular brittle fracture. Tin lamellare-BiIn interface and BiIn

dendrite stem may act as a crack propagation path during brittle fracture.

### Acknowledgements

Financial support from the Natural Sciences and Engineering Research Council of Canada is gratefully acknowledged. Appreciation is also expressed for useful suggestions by Professor J. W. Rutter and Professor Z. Wang of the University of Toronto.

### References

1. G. MOTOYASU, K. KADOWAKI, H. SODA and A. McLEAN, *J. Mater. Sci.* **34** (1999) 3893.
2. A. OHNO, *J. Metals* **38** (1986) 14.
3. H. SODA, G. MOTOYASU, A. McLEAN and Z. WANG, *J. Mater. Sci.* **30** (1995) 5438.
4. M. A. RUGGIERO and J. W. RUTTER, *Mater. Sci. Technol.* **11** (1995) 136.
5. *Idem.*, *ibid.* **14** (1998) 177.
6. S. SENGUPTA, H. SODA, A. McLEAN and J. W. RUTTER, *Metall. and Mater. Trans. A* **31A** (2000) 239.
7. D. BARAGAR, M. SAHOO and R. W. SMITH, in "Solidification and Casting of Metals" (The Metals Society, London, UK, 1979) p. 88.
8. H. W. KERR and W. C. WINEGARD, *Can. Met. Quarterly* **6** (1967) 55.
9. S. D. BAGHERI and J. W. RUTTER, *Mater. Sci. Technol.* **13** (1997) 541.
10. H. C. DEGROH, III and V. LAXMANAN, *Metall. Trans. A* **19A** (1988) 2651.
11. P. J. WRAY, *J. Appl. Phys.* **40** (1969) 4018.
12. J. GLAZER, *Int. Mater. Reviews* **40** (1995) 65.

Received 11 July

and accepted 21 November 2001